Available online at www.sciencedirect.com
SCIENCE DIRECT®
Journal of Inorganic Biochemistry 99 (2005) 530–537
Journal of Inorganic Biochemistry
www.elsevier.com/locate/jinorgbio

Interaction of polypyridyl ruthenium (II) complex containing asymmetric ligand with DNA

Yun-Jun Liu [a,b], Hui Chao [a,c,*], Li-Feng Tan [a], Yi-Xian Yuan [a], Wei Wei [a], Liang-Nian Ji [a,b,*]

[a] Department of Chemistry, Sun Yat-Sen University, Guangzhou 510275, PR China
[b] The Key Laboratory of Gene Engineering of Ministry of Education, Sun Yat-Sen University, XinGangXilu 135, Guangzhou 510275, PR China
[c] State Key Laboratory of Coordination Chemistry, Nanjing University, Nanjing 210093, PR China

Received 6 July 2004; received in revised form 20 October 2004; accepted 22 October 2004
Available online 21 November 2004

Abstract

A novel asymmetric bidentate ruthenium (II) complex, $[Ru(bpy)_2(PYNI)]^{2+}$ (bpy = 2,2′-bipyridine, PYNI = 2-(2′-pyridyl)naphthoimidazole), has been synthesized and characterized by elemental analysis, ES-MS (electrospray mass spectra) and ^1H NMR. The electrochemical behaviors of this complex were studied by cyclic voltammetry. DNA interaction studies suggest that $[Ru(bpy)_2(PYNI)]^{2+}$ binds to calf thymus DNA (CT-DNA) in an intercalative mode. Interestingly, this new Ru(II) complex has also been found to promote cleavage of plasmid pBR 322 DNA from the supercoiled form I to the open circular form II upon irradiation.

Keywords: Ruthenium complexes; DNA binding; Photocleavage

1. Introduction

The interaction of ruthenium (II) polypyridyl complexes with DNA has attracted considerable interest during the past decades. An understanding of how these small molecules bind to DNA will be potentially useful in the design of new drugs and highly sensitive spectroscopic and reactive probes and diagnostic reagents [1–4]. However, most of these studies have focused on the complexes with symmetric aromatic ligands such as $[Ru(bpy)_2(dppz)]^{2+}$ and $[Ru\text{-}(phen)_2(dppz)]^{2+}$ (bpy = 2,2′-bipyridine, phen = 1,10-phenanthroline, dppz = dipyridophenazine) [5–14]. Nevertheless, understanding more details of the structure of DNA may require the preparation of more structurally analogous complexes with different shape and electronic properties and investigation of the DNA binding behavior.

Recently, a few of ruthenium (II) complexes containing asymmetric ligands have been synthesized, and some of them also exhibit interesting properties upon binding to DNA [15–20]. In attempt to obtain more insight into the DNA-binding properties of ruthenium (II) complexes with asymmetric ligands, we synthesized and characterized a novel asymmetric bidentate ligand 2-(2′-pyridyl)naphthoimidazole (PYNI) and its ruthenium (II) complex. The DNA-binding and photocleavage properties of the ruthenium (II) complex were explored by spectroscopic methods and viscosity measurement. The photocleavage behaviors of the ruthenium (II) complex toward pBR 322 DNA were also investigated. In the complex two bpy are used as co-complexation ligands,

* Corresponding author. Tel.: +86 20 8411 4091; fax: +86 20 8403 5497.
E-mail address: ceschao@yahoo.com (H. Chao).

0162-0134/$ - see front matter © 2004 Elsevier Inc. All rights reserved.
doi:10.1016/j.jinorgbio.2004.10.030

because bpy has been previously demonstrated to be only minimally efficient at inducing intercalative binding with DNA [21], allowing us to focus on the influence of the side face of PYNI on the interaction.

2. Experimental

2.1. Materials

All reagents and solvents were purchased commercially and used without further purification unless otherwise noted. Tris–HCl buffer (5 mM Tris–HCl, 50 mM NaCl, pH 7.2, Tris = Tris(hydroxymethyl)aminomethane) solution was prepared using doubly distilled water. Calf thymus DNA (CT-DNA) was obtained from the Sino-American Biotechnology Company. A solution of calf thymus DNA in the buffer gave a ratio of UV absorbance at 260 and 280 nm of ca. 1.8–1.9:1, indicating that the DNA was sufficiently free of protein [22]. The DNA concentration per nucleotide was determined by absorption spectroscopy using the molar absorption coefficient (6600 $M^{-1}\,cm^{-1}$) at 260 nm [23].

2.2. Synthesis

2.2.1. Synthesis of PYNI

A mixture of 2-cyanopyridine (0.42 g, 4 mmol), 2,3-diaminonaphthalene (0.63 g, 4 mmol) and polyphosphoric acid (5 cm^3) was heated at 240 °C for 4 h. The reaction mixture was then cooled to room temperature and poured into water (50 cm^3). The solution was neutralized with a 25% NH_3 solution. A yellow precipitate was obtained and recrystallized from ethanol, then dried in vacuo. Yield: 76%. (Found: C, 78.2; H, 4.4; N, 16.8. Calc. For $C_{16}H_{11}N_3$: C, 78.4; H, 4.5; N, 17.1%). ^1H NMR (ppm, DMSO-d_6): 13.20 (s, 1H), 8.79 (d, 1H, $J = 9.0$ Hz), 8.46 (d, 1H, $J = 8.0$ Hz), 8.14 (s, 2H), 8.05 (t, 1H, $J = 7.5$ Hz), 8.01 (dd, 2H, $J_1 = 3.5$ Hz, $J_2 = 3.0$ Hz), 7.59 (t, 1H, $J = 5.0$ Hz), 7.37 (m, 2H). FAB-MS: $m/z = 246$ [M + 1].

2.2.2. Synthesis of [Ru(bpy)$_2$(PYNI)](ClO$_4$)$_2$ (1)

A mixture of *cis*-$[Ru(bpy)_2Cl_2]\cdot 2H_2O$ [24] (0.10 g, 0.2 mmol) and PYNI (0.049 g, 0.2 mmol) in ethylene glycol (15 cm^3) was refluxed under argon for 6 h to give a clear red solution. Upon cooling, a brown red precipitate was obtained by dropwise addition of saturated aqueous $NaClO_4$ solution. The crude product was purified by column chromatography on a neutral alumina with CH_3CN–toluene (2:1, v/v) as eluant. The mainly brown red band was collected. The solvent was removed under reduced pressure and a brown red powder was obtained. Yield: 64% (Found: C, 50.2; H, 3.5; N, 11.3. Calc. for $C_{36}H_{27}N_7Cl_2O_8Ru$: C, 50.4; H, 3.2; N, 11.4%). ^1H NMR (ppm, DMSO-d_6): 8.86 (d, 1H, $J = 8.5$ Hz), 8.83 (d, 1H, $J = 8.5$ Hz), 8.81 (d, 1H, $J = 8.5$ Hz), 8.69 (d, 1H, $J = 9.0$ Hz), 8.46 (d, 1H, $J = 8.5$ Hz), 8.34 (t, 1H, $J = 6.5$ Hz), 8.28 (s, 1H), 8.16 (t, 1H, $J = 7.0$ Hz), 8.08 (m, 2H), 8.00 (m, 3H), 7.87 (d, 1H, $J = 7.5$ Hz), 7.85 (t, 1H, $J = 7.5$ Hz), 7.73 (d, 1H, $J = 7.0$ Hz), 7.68 (m, 2H), 7.56 (t, 1H, $J = 6.5$ Hz), 7.53 (d, 1H, $J = 5$ Hz), 7.45 (m, 2H), 7.16 (m, 2H), 7.12 (d, 1H, $J = 6.5$ Hz), 5.80 (s, 1H). ES-MS (CH_3OH): m/z 657 ($[M - 2ClO_4 - H]^+$), 329 ($[M - 2ClO_4]^{2+}$).

Caution! Perchlorate salts of metal complexes with organic ligands are potentially explosive, and only small amounts of the material should be prepared and handled with great care.

2.3. Physical measurements

Microanalysis (C, H, and N) was carried out with a Perkin–Elmer 240Q elemental analyzer. Fast atom bombardment (FAB) mass spectra were measured on a VG ZAB-HS spectrometer in a 3-nitrobenzyl alcohol matrix. Electrospray mass spectra (ES-MS) were recorded on a LCQ system (Finnigan MAT, USA) using methanol as mobile phase. The spray voltage, tube lens offset, capillary voltage and capillary temperature were set at 4.50 kV, 30.00, 23.00 V and 200 °C, respectively, and the quoted m/z values are for the major peaks in the isotope distribution. ^1H NMR spectra were recorded on a Varian-500 spectrometer. All chemical shifts were given relative to tetramethylsilane (TMS). UV–visible (UV–Vis) spectra were recorded on a Shimadzu UV-3101PC spectrophotometer at room temperature. Cyclic voltammetric measurements were performed on a CHI 660A Electrochemical Workstation. The supporting electrolyte was 0.1 M tetrabutylammonium perchlorate in acetonitrile freshly distilled from phosphorus pentaoxide. The sample (5×10^{-4} M) was purged with nitrogen prior to measurements. A standard three-electrode system comprising of platinum microcylinder working electrode, platinum-wire auxiliary electrode and a saturated calomel reference electrode (SCE) was used.

2.4. DNA-binding and cleavage experiments

The DNA-binding and cleavage experiments were performed at room temperature. The absorption titrations of ruthenium (II) complexes in buffer (5 mM Tris–HCl, 50 mM NaCl, pH 7.2) were performed by using a fixed ruthenium concentration to which increments of the DNA stock solution were added. Ruthenium solutions employed were 20 μM in concentration and calf thymus DNA was added to a ratio of 4:1 [DNA]/[Ru]. Ruthenium–DNA solutions were allowed to incubate for 10 min before the absorption spectra

were recorded. The intrinsic binding constants K_b of Ru(II) complexes to DNA were calculated from Eq. (1) [25].

$$[\mathrm{DNA}]/(\varepsilon_a - \varepsilon_f) = [\mathrm{DNA}]/(\varepsilon_b - \varepsilon_f) + 1/[K_b(\varepsilon_b - \varepsilon_f)], \quad (1)$$

where [DNA] is the concentration of DNA in base pairs, ε_a, ε_f and ε_b correspond to the apparent absorption coefficient A_{obsd}/[Ru], the extinction coefficient for the free ruthenium complex and the extinction coefficient for the ruthenium complex in the fully bound form, respectively. In plots of [DNA]/($\varepsilon_a - \varepsilon_f$) versus [DNA], K_b is given by the ratio of slope to the intercept.

Thermal denaturation studies were carried out with a Perkin–Elmer Lambda 35 spectrophotometer equipped with a Peltier temperature-controlling programmer (±0.1 °C). The absorbance at 260 nm was continuously monitored for solutions of CT-DNA (100 μM) in the absence and presence of the Ru(II) complex (30 μM). The temperature of the solution was increased by 1 °C min^{-1}.

For the steady-state emission quenching experiment using $[Fe(CN)_6]^{4-}$ as quencher, according to the classical Stern–Volmer equation (2) [26]

$$I_0/I = 1 + Kr, \quad (2)$$

where I_0 and I are the luminescence intensities in the absence and presence of $[Fe(CN)_6]^{4-}$, respectively. K is a linear Stern–Volmer quenching constant dependent on the ratio of the bound concentration of Ru(II) complex to the concentration of DNA. r is the concentration of the quencher $[Fe(CN)_6]^{4-}$. In the plot of I_0/I vs. r, the Stern–Volmer quenching constant K is derived from the slope.

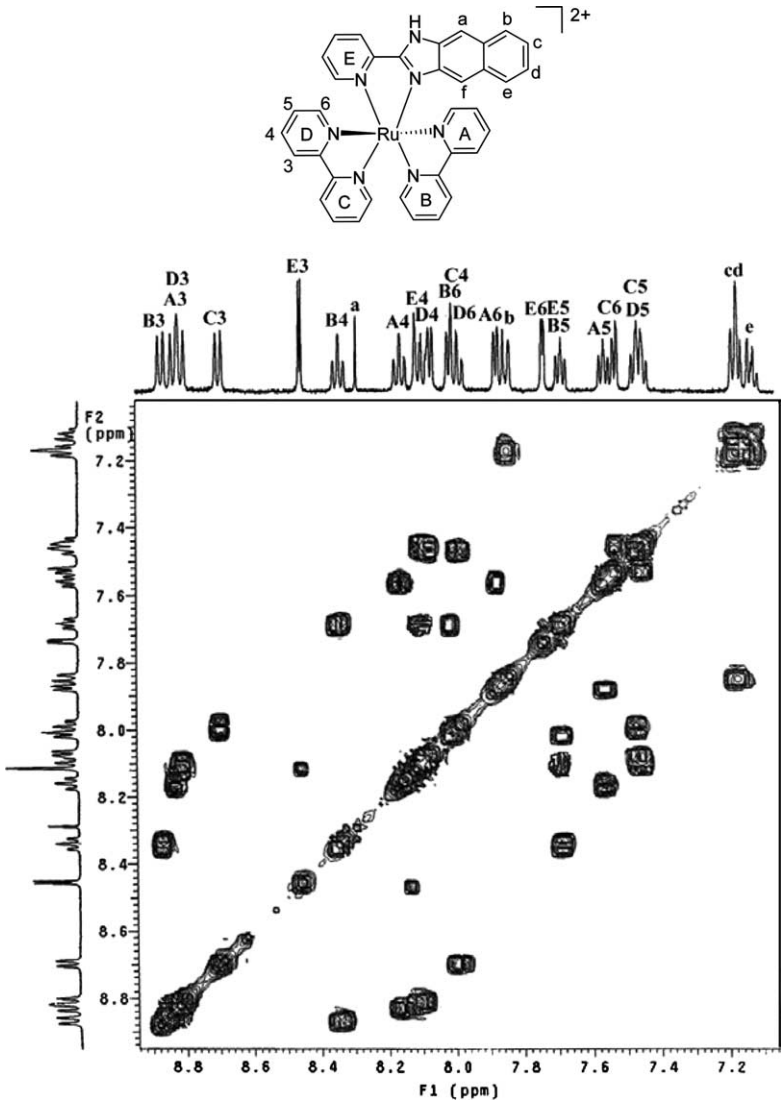

Fig. 1. ^1H–^1H COSY spectra of $[Ru(bpy)_2(PYNI)]^{2+}$ in $(CD_3)SO$ (500 MHz).

Viscosity measurements were carried out using an Ubbelodhe viscometer maintained at a constant temperature at 29.0 ± 0.1 °C in a thermostatic bath. DNA samples approximately 200 bp in average length were prepared by sonicating in order to minimize complexities arising from DNA flexibility [27]. Flow time was measured with a digital stopwatch, and each sample was measured three times, and an average flow time was calculated. Data were presented as $(\eta/\eta_0)^{1/3}$ versus binding ratio [28], where η is the viscosity of DNA in the presence of complex and η_0 is the viscosity of DNA alone.

For the gel electrophoresis experiment, supercoiled pBR 322 DNA (0.1 μg) was treated with the Ru(II) complex in the buffer (50 mM Tris–HCl, 18 mM NaCl, pH 7.2), and the solution was then irradiated at room temperature with a UV lamp (365 nm, 10 W). The samples were analyzed by electrophoresis for 1 h at 100 V on a 1% agarose gel in Tris–HCl buffer. The gel was stained with 1 μg ml^{-1} ethidium bromide and photographed under UV light.

3. Results and discussion

3.1. Characterization

The ^1H–^1H COSY (correlated spectroscopy) NMR spectrum of $[Ru(bpy)_2(PYNI)]^{2+}$ in hexadeuterodimethyl sulfoxide (DMSO-d_6) is shown in Fig. 1. It is interesting to note that, due to the asymmetry of the complex, the protons in different positions (H3, H4, H5, H6) on different pyridine rings (A, B, C, D, E) are distinguished as defined in the structure. The chemical shifts of the protons on the PYNI naphthyl ring, however, separate at higher field, especially H_f at 5.80 ppm because of the ring current effect with the naphthyl ring facing pyridine A in the complex.

The electrochemical behavior of $[Ru(bpy)_2(PYNI)]^{2+}$ has been studied in acetonitrile by cyclic voltammetry. The Ru(II) complex exhibits well-defined waves corresponding to the metal-based oxidation and successive ligand-based reduction in the sweep rang from −2.0 to 2.0 V (Fig. 2). The anodic and cathodic peak separations vary from 61 to 72 mV and are nearly independent to scan rate, indicating that the processes are reversible and belong to one-electron transfer. As expected, the oxidation potential 1.16 V (versus SCE) of $[Ru(bpy)_2(PYNI)]^{2+}$ is more negative than that of $[Ru(bpy)_3]^{2+}$ (1.28 V) [29] due to the donor capacity of the coordinated imidazole. For the two reversible reduction waves observed in the cyclic voltammogram (−1.44 and −1.68 V), by comparing with the redox behaviors of $[Ru(bpy)_3]^{2+}$ and related complexes [30,31], they are characteristic of the two bpy ligands.

3.2. Absorption spectroscopic studies

The absorption spectrum of $[Ru(bpy)_2(PYNI)]^{2+}$ mainly consists of three resolved bands in range 200–600 nm. The bands at 286 nm is attributed to intraligand (IL) π–π* transitions, the band at 352 nm is attributed to the π–π* transition and the lowest energy bands at 470 nm is assigned to the metal-to-ligand charge transfer (MLCT) transitions by comparison with the spectra of

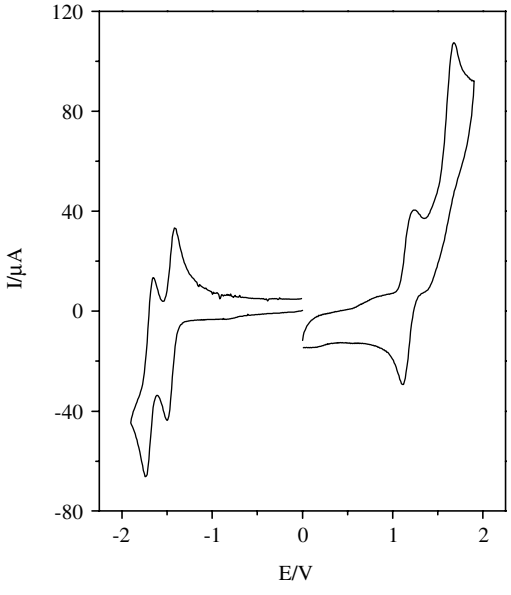

Fig. 2. Cyclic voltammogram of $[Ru(bpy)_2(PYNI)]^{2+}$ in CH_3CN.

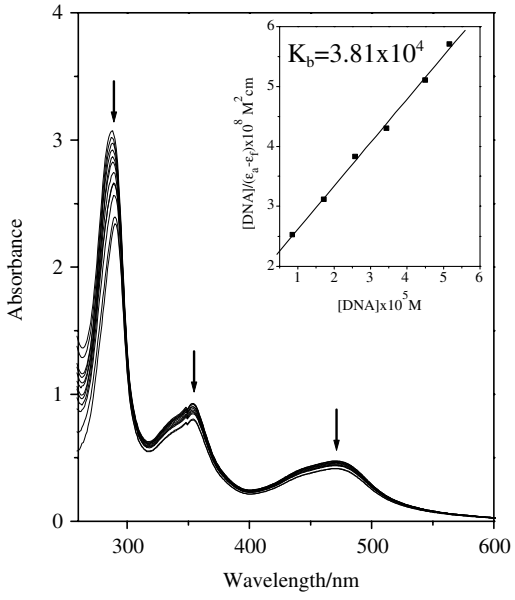

Fig. 3. Absorption spectra of $[Ru(bpy)_2(PYNI)]^{2+}$ in the presence of increasing amounts of DNA with subtraction of the DNA absorbance ([Ru] = 20 μM, [DNA] = 0–80 μM). The arrow shows the absorbance changes on increasing DNA concentration.

other polypyridyl Ru(II) complexes [30,31]. The electronic spectral traces of the Ru(II) complex titrated at room temperature with DNA are shown in Fig. 3. As the DNA concentration is increased, for complex $[Ru(bpy)_2(PYNI)]^{2+}$, the hypochromism in the IL band reaches as high as 22.5% at 286 nm with a red shift of 4 nm; the MLCT band at 470 nm shows hypochromism by about 12.8% and a red shift of 3 nm under the same experimental conditions. Obviously, these spectral characteristics suggest that the complex in our paper interact with DNA most likely through a mode that involves a stacking interaction between the aromatic chomophore and the base pairs of DNA. In order to further illustrate the binding strength of the complex, the intrinsic binding constants K_b of it with CT-DNA was determined by monitoring the changes of absorbance in the MLCT (470 nm) band with increasing concentration of DNA. The intrinsic binding constant K_b of the complex obtained was 3.81×10^4 M^{-1}, from the decay of the absorbance. This value is comparable to that of those so-called DNA–intercalative Ru(II) complexes (1.1×10^4 –4.8×10^4 M^{-1}) [16,32]. The results of absorption spectroscopic studies indicate that complex $[Ru(bpy)_2(PYNI)]^{2+}$ binds strongly to DNA by intercalation.

3.3. Thermal denaturation study

Thermal behaviors of DNA in the presence of complexes can give insight into their conformational changes when temperature is raised, and offer information about the interaction strength of complexes with DNA. It is well known that when the temperature in the solution increases, the double-stranded DNA gradually dissociates to single strands, and generates a hyperchromic effect on the absorption spectra of DNA bases (λ_{max} = 260 nm). In order to identify this transition process, the melting temperature T_m, which is defined as the temperature where half of the total base pairs is unbonded, is usually introduced. According to the literatures [33–35], the intercalation of natural or synthesized organics and metallointercalators generally results in a considerable increase in melting temperature (T_m). Here, a DNA (100 μM) melting experiment revealed that T_m of calf thymus DNA is 75.6 ± 0.2 °C in the absence of the complex (Fig. 4). However, with addition of $[Ru(bpy)_2(PYNI)]^{2+}$ (30 μM), the T_m of the DNA increase dramatically to 83.0 ± 0.2 °C. The large increase (~7.5 °C) in T_m of the latter is comparable to that observed for classical intercalators [33–35].

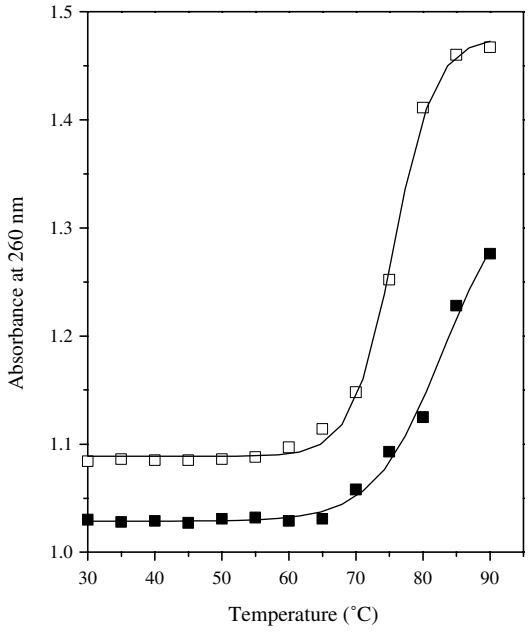

Fig. 4. Melting temperature curves of DNA in the absence (□) and presence of $[Ru(bpy)_2(PYNI)]^{2+}$ (■). [Ru] = 30 μM, [DNA] = 100 μM.

3.4. Luminescence spectroscopic study

Complex $[Ru(bpy)_2(PYNI)]^{2+}$ can emit luminescence in Tris buffer at room temperature, with maxima at about 583 nm, excited in 464 nm. Its interaction with CT-DNA was monitored with luminescence. The results of emission titrations for $[Ru(bpy)_2(PYNI)]^{2+}$ with CT-DNA are illustrated in Fig. 5. Upon addition of CT-DNA, the emission intensity of the Ru(II) complex increases to around 2.9 times larger than the original and saturates at a ratio of [DNA]/[Ru] = 21.5. This implies that $[Ru(bpy)_2(PYNI)]^{2+}$ can interact with CT-DNA and be protected by DNA efficiently, since the hydrophobic environment inside the DNA helix reduces the accessibility of solvent water molecules to the complex and the complex mobility is restricted at the binding site, leading to decrease of the vibrational modes of relaxation. We can also derive the binding constant of the complex interacting with DNA from the emission spectra using the luminescence titration method. The binding data obtained from the emission spectra were fitted using the McGhee and von Hippel equation [36] to acquire the binding parameters. The intrinsic binding constant K_b of 4.32 (± 0.2) $\times 10^4$ M^{-1} for complex was determined. Comparing with that obtained from absorption spectra, although the binding constant obtained from luminescence titration with McGhee–von Hippel method is different from that obtained absorption with the method suggested by Wolfe et al. [25], this difference between the two sets of binding constants should be caused by the different spectroscopy and different calculation method. The binding site, n, was 2.32 (±0.05) base pairs for complex, which is also similar to those of many Ru(II) polypyridine complexes [37].

Steady-state emission quenching experiment using $[Fe(CN)_6]^{4-}$ as quencher is also used to observe the binding of $[Ru(bpy)_2(PYNI)]^{2+}$ with CT-DNA, and the known DNA intercalator $[Ru(bpy)_2(atatp)]^{2+}$ [38]

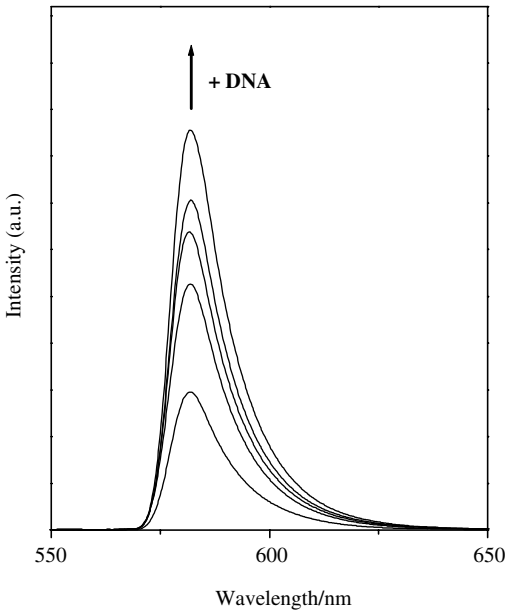

Fig. 5. Emission spectra of $[Ru(bpy)_2(PYNI)]^{2+}$ in Tris–HCl buffer in the absence and presence of CT-DNA. Arrow shows the intensity change upon increasing DNA concentrations.

is selected as reference. As illustrated in Fig. 6, in the absence of DNA, the Ru(II) complex is efficiently quenched by $[Fe(CN)_6]^{4-}$, resulting in a linear Stern–Volmer plot with a slope of 2.45 and 1.84 for complexes $[Ru(bpy)_2(PYNI)]^{2+}$ and $[Ru(bpy)_2(atatp)]^{2+}$. In the presence of DNA, however, the Stern–Volmer plot changes drastically, and the efficiency of quenching (slope 0.18 and 0.13 for $[Ru(bpy)_2(PYNI)]^{2+}$ and $[Ru(bpy)_2(atatp)]^{2+}$, respectively) of the Ru(II) complex bound to DNA by $[Fe(CN)_6]^{4-}$ is decreased relative to that of the free Ru(II) complex. This also reflects the strong DNA-binding affinity of $[Ru(bpy)_2(PYNI)]^{2+}$ and may be explained by the fact that the bound cations of the Ru(II) complex are protected from the anionic water-bound quencher by the negative DNA phosphate backbone, hindering quenching the emission of bound complexes [21,39]. The slope can be taken as a measure of binding affinity, a large slope corresponding to poor protection and low binding [21,39]. Although the shapes of $[Ru(bpy)_2(PYNI)]^{2+}$ and $[Ru(bpy)_2(atatp)]^{2+}$ are different, the slope of $[Ru(bpy)_2(PYNI)]^{2+}$ is similar to that of $[Ru(bpy)_2(atatp)]^{2+}$. The experimental results suggest that complex $[Ru(bpy)_2(PYNI)]^{2+}$ could bind DNA in classical intercalation mode.

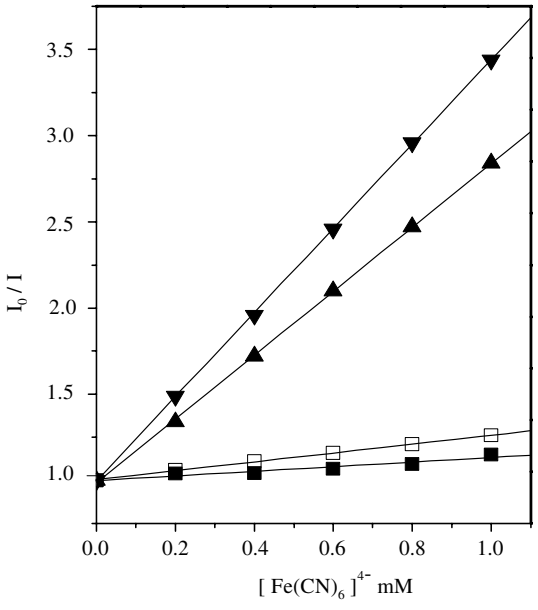

Fig. 6. Emission quenching with $[Fe(CN)_6]^{4-}$ for free (▼) or DNA-bound (□) $[Ru(bpy)_2(PYNI)]^2$ and free (▲) or DNA-bound (■) $[Ru(bpy)_2(actatp)]^{2+}$ ([Ru] = 4 μM, [DNA]/[Ru] = 40).

3.5. Viscosity measurement

In fact, optical photophysical probes generally provide necessary but not sufficient clues to support a binding mode. Viscosity measurements that are sensitive to length change of DNA are regarded as the least ambiguous and the most critical tests of binding mode in solution in the absence of crystallographic structural data or NMR spectra [40,41]. It is popularly accepted that a classical intercalation mode results in lengthening the DNA helix, as base pairs are separated to accommodate the binding ligand, leading to the increase of DNA viscosity. In contrast, a partial and/or non-classical intercalation of ligand could bend (or kink) the DNA helix, reduce its effective length and, concomitantly, its viscosity [40,41]. In order to further elucidate the binding mode of the present complex, viscosity measurements were carried out on calf thymus DNA by varying the concentration of the added complex. The effects of the complex $[Ru(bpy)_2(PYNI)]^{2+}$, together with $[Ru(bpy)_2(dppz)]^{2+}$ on the viscosity of rod-like DNA were shown in Fig. 7. As expected, $[Ru(bpy)_2(dppz)]^{2+}$, a proved DNA intercalator, increases the relative specific viscosity for the lengthening of the DNA double helix resulting from intercalation. Upon increasing concentration of $[Ru(bpy)_2(PYNI)]^{2+}$, the viscosity of the DNA also increase steadily but is smaller than those bound with $[Ru(bpy)_2(dppz)]^{2+}$. The results indicate that $[Ru(bpy)_2(PYNI)]^{2+}$ can intercalate into DNA base pairs too, which is consistent with the spectroscopic results above.

3.6. Photoactivated cleavage of pBR 322 DNA by Ru(II) complex

The cleavage reaction on plasmid DNA can be monitored by agarose gel electrophoresis. When circular plasmid DNA is subject to electrophoresis, relatively fast migration will be observed for the intact supercoil

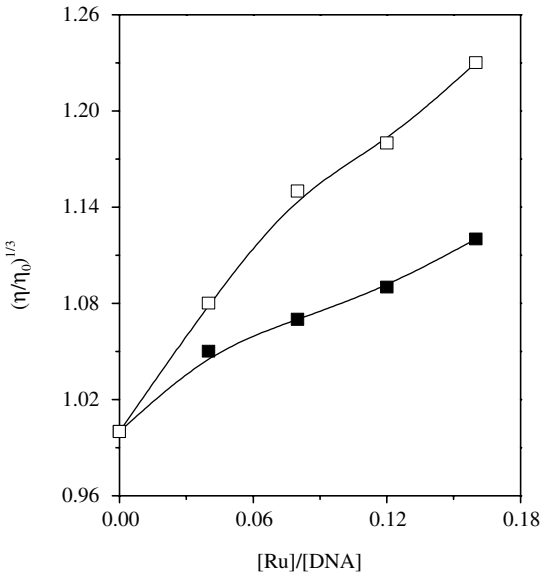

Fig. 7. Effect of increasing amounts of the complexes of $[Ru(bpy)_2(dppz)]^{2+}$ (□) and $[Ru(bpy)_2(PYNI)]^{2+}$ (■) on the relative viscosity of calf thymus DNA at 29 (±0.1) °C. The total concentration of DNA is 0.5 mM.

form (Form I). If scission occurs on one strand (nicking), the supercoil will relax to generate a slower-moving open circular form (Form II). If both strands are cleaved, a linear form (Form III) that migrates between Form I and Form II will be generated [42]. Fig. 8 shows gel electrophoresis separation of pBR 322 DNA after incubation with $[Ru(bpy)_2(PYNI)]^{2+}$ and irradiation at 365 nm. No DNA cleavage was observed for controls in which the complex was absent (lane 0), or incubation of the plasmid with the Ru(II) complex in dark (data not presented). With increasing concentration of the Ru(II) complex (lanes 1–4), the amount of Form I of pBR 322 DNA diminish gradually, whereas Form II increases. At the concentration of 40 μM, $[Ru(bpy)_2(PYNI)]^{2+}$ can almost promoting the complete conversion of DNA from the form I to form II (lane 4). Although DNA photocleavage by $[Ru(phen)_3]^{2+}$ and other Ru(II) complexes has been reported to involve an $^1O_2$-based mechanism

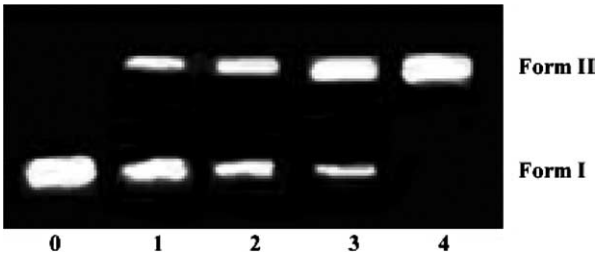

Fig. 8. Photoactivated cleavage of pBR 322 DNA in the presence of $[Ru(bpy)_2(PYNI)]^{2+}$ and light. Lane 0, DNA alone; lanes 1–4, in the different concentration of Ru(II) complex: (1) 10; (2) 20; (3) 30; (4) 40 μM.

[43,44], the mechanism of their action involved in the efficient DNA photocleavage by the new Ru(II) complex observed in this study has not yet been explored in detail.

4. Conclusions

A newly asymmetric ruthenium (II) complex $[Ru(bpy)_2(PYNI)]^{2+}$ has been synthesized and characterized. Photophysical and viscometric studies have demonstrated that this complex can intercalate into DNA base pairs via its extended, planar ligands. In addition, this Ru(II) complex has been found to promote the single-stranded cleavage of plasmid pBR 322 DNA upon irradiation.

Acknowledgments

We are grateful to the National Natural Science Foundation of China, the Natural Science Foundation of Guangdong Province, the State Key Laboratory of Coordination Chemistry in Nanjing University and Research Fund of Royal of Chemistry, UK for their financial supports.

References

[1] A. Sigel, H. Sigel (Eds.), Metal Ions in Biological Systems, vol. 33, Marcel Dekker, New York, 1996.
[2] K.E. Erkkila, D.T. Odom, J.K. Barton, Chem. Rev. 99 (1999) 2777–2795.
[3] L.-N. Ji, X.-H. Zou, J.-G. Liu, Coord. Chem. Rev. 216–217 (2001) 513–536.
[4] L.-N. Ji, Q.-L. Zhang, H. Chao, Chin. Sci. Bull. 46 (2001) 1332–1337.
[5] A.E. Friedman, J.C. Chambron, J.-P. Sauvage, N.J. Turro, J.K. Barton, J. Am. Chem. Soc. 112 (1990) 4960–4962.
[6] R.M. Hartshorn, J.K. Barton, J. Am. Chem. Soc. 114 (1992) 5919–5925.
[7] C. Hiort, P. Lincoln, B. Nordén, J. Am. Chem. Soc. 115 (1993) 3448–3454.
[8] E. Tuite, P. Lincoln, B. Nordén, J. Am. Chem. Soc. 119 (1997) 239–240.
[9] A. Ambroise, B.G. Maiya, Inorg. Chem. 39 (2000) 4264–4272.
[10] J.G. Collins, A.D. Sleeman, J.R. Aldrich-Wright, I.D. Greguric, T.W. Hambley, Inorg. Chem. 37 (1998) 3133–3141.
[11] J.G. Collins, J.R. Aldrich-Wright, I.D. Greguric, P.A. Pellegrini, Inorg. Chem. 38 (1999) 5502–5509.
[12] J.-Z. Wu, B.-H. Ye, L. Wang, L.-N. Ji, J.-Y. Zhou, R.-H. Li, Z.-Y. Zhou, J. Chem. Soc., Dalton Trans. (1997) 1395–1401.
[13] Q.-X. Zhen, B.-H. Ye, Q.-L. Zhang, J.-G. Liu, H. Li, L.-N. Ji, L. Wang, J. Inorg. Biochem. 76 (1999) 47–53.
[14] J.-G. Liu, B.-H. Ye, Q.-L. Zhang, X.-H. Zou, Q.-X. Zhen, X. Tian, L.-N. Ji, J. Biol. Inorg. Chem. 5 (2000) 119–128.
[15] X.-H. Zou, B.-H. Ye, H. Li, J.-G. Liu, Y. Xiong, L.-N. Ji Soc., J. Chem., Dalton Trans. (1999) 1423–1428.
[16] X.-H. Zou, B.-H. Ye, H. Li, Q.-L. Zhang, H. Chao, J.-G. Liu, L.-N. Ji, J. Biol. Inorg. Chem. 6 (2001) 143–150.

[17] H. Deng, J.-W. Cai, H. Xu, H. Zhang, L.-N. Ji, J. Chem. Soc., Dalton Trans. 3 (2003) 325–330.
[18] H. Chao, W.-J. Mei, Q.-W. Huang, L.-N. Ji, J. Inorg. Biochem. 92 (2002) 165–170.
[19] C.-W. Jiang, H. Chao, H. Li, L.-N. Ji, J. Inorg. Biochem. 93 (2003) 247–255.
[20] X.-L. Hong, H. Chao, L.-J. Lin, K.-C. Zheng, H. Li, X.-L. Wang, F.-C. Yun, L.-N. Ji, Helv. Chim. Acta 87 (2004) 1180–1193.
[21] C.V. Kumar, N.J. Turro, J.K. Barton, J. Am. Chem. Soc. 107 (1985) 5518–5523.
[22] J. Marmur, J. Mol. Biol. 3 (1961) 208–211.
[23] M.F. Reichmann, S.A. Rice, C.A. Thomas, P. Doty, J. Am. Chem. Soc. 76 (1954) 3047–3053.
[24] B.P. Sullivan, D.J. Salmon, T.J. Meyer, Inorg. Chem. 17 (1978) 3334–3341.
[25] A. Wolf, G.H. Shimer Jr., T. Meehan, Biochemistry 26 (1987) 6392–6396.
[26] J.R. Lakowicz, G. Webber, Biochemistry 12 (1973) 4161–4170.
[27] J.B. Chaires, N. Dattagupta, D.M. Crothers, Biochemistry 21 (1982) 3933–3940.
[28] G. Cohen, H. Eisenberg, Biopolymers 8 (1969) 45–49.
[29] T. Matsumura-Inoue, J. Electroanal. Chem. 95 (1979) 109–112.
[30] M. Haga, Inorg. Chim. Acta 75 (1983) 29–35.
[31] S. Baitalik, U. Flörke, K. Nag, J. Chem. Soc., Dalton Trans. (1999) 719–727.
[32] A.M. Pyle, J.P. Rehmann, R. Meshoyrer, C.V. Kumar, N.J. Turro, J.K. Barton, J. Am. Chem. Soc. 111 (1989) 3051–3058.
[33] M.J. Waring, J. Mol. Biol. 13 (1965) 269–274.
[34] J.M. Kelly, A.B. Tossi, D.J. McConell, C. OhUigin, Nucleic Acids Res. 13 (1985) 6017–6034.
[35] G.A. Neyhart, N. Grover, S.R. Smith, W.A. Kalsbeck, T.A. Fairly, M. Cory, H.H. Thorp, J. Am. Chem. Soc. 115 (1993) 4423–4428.
[36] J.D. McGhee, P.H. von Hippel, J. Mol. Biol. 86 (1974) 469–475.
[37] R.J. Morgan, S. Chatterjee, A.D. Baker, T.C. Strekas, Inorg. Chem. 30 (1991) 2687–2692.
[38] Q.-X. Zhen, Q.-L. Zhang, J.-G. Liu, B.-H. Ye, L.-N. Ji, L. Wang, J. Inorg. Biochem. 78 (2000) 293–298.
[39] J.K. Barton, J.M. Goldberg, C.V. Kumar, N.J. Turro, J. Am. Chem. Soc. 108 (1986) 2081–2088.
[40] S. Satyanarayana, J.C. Dabroniak, J.B. Chaires, Biochemistry 31 (1992) 9319–9324.
[41] S. Satyanaryana, J.C. Daborusak, J.B. Chaires, Biochemistry 32 (1993) 2573–2584.
[42] J.K. Barton, A.L. Raphael, J. Am. Chem. Soc. 106 (1984) 2466–2468.
[43] H.Y. Mei, J.K. Barton, Proc. Natl. Acad. Sci. USA 85 (1988) 1339–1347.
[44] A. Hergueta-Bravo, M.E. Jiménez-Hernández, F. Montero, E. Oliveros, G. Orellana, J. Phys. Chem. B 106 (2002) 4010–4017.